Nat Hazards (2018) 93:67–88
https://doi.org/10.1007/s11069-018-3289-9

ORIGINAL PAPER

Design rainfall estimation: comparison between GEV and LP3 distributions and at-site and regional estimates

Evan Hajani[1] · Ataur Rahman[1]

Received: 15 November 2016 / Accepted: 25 March 2018 / Published online: 29 March 2018

Abstract Design rainfall, often known as intensity–frequency–duration (IFD) data, is an important input in rainfall runoff modelling exercise. IFD data are derived by fitting a probability distribution to observed rainfall data. Although there are many researches on IFD curves in the literature, there is a lack of systematic comparison among the IFD curves obtained by different distributions and methods. This study compares the latest IFD curves in Australia, published in 2013, as a part of the new Australian rainfall and runoff (ARR) with the at-site IFD curves to examine the expected degree of variation between the at-site and regional IFD data. Ten pluviography stations from eastern New South Wales (NSW) are selected for this study. The IFD curves generated by the two most commonly adopted probability distributions, generalised extreme value (GEV) and log Pearson type 3 (LP3) distributions are also compared. Empirical and polynomial regression methods in smoothing the IFD curves are compared. Based on the three goodness-of-fit tests, it has been found that both GEV and LP3 distributions fit the annual maximum rainfall data (at 1% significance level) for the ten selected stations. The developed IFD curves based on the second-degree polynomial present better fitting than the empirical method. It has been found that the ARR87 and ARR13 IFD curves are generally higher than the at-site IFD curves derived here. The median difference between the at-site and regional ARR-recommended IFD curves is in the range of 13–19%. It is expected that the outcomes of this research will provide better guidance in selecting the correct IFD data for a given application in NSW. The methodology developed here can be adapted to other parts of Australia and other countries.

Keywords Rainfall · Intensity · Duration · Frequency · Generalised extreme value distribution · Log Pearson type 3 · Goodness-of-fit test

✉ Ataur Rahman
a.rahman@westernsydney.edu.au

[1] School of Computing, Engineering and Mathematics, Western Sydney University, Locked Bag 1797, Penrith, NSW 2751, Australia

1 Introduction

Design rainfall in the form of intensity, frequency and duration (IFD) information is one of the most commonly used data in planning, designing, development and risk assessment of water resources engineering projects (BOM 2016). The IFD represent a functional relationship among three important parameters, average rainfall intensity, duration and return period. Due to the paramount importance of IFD curves, it has been widely researched previously (e.g. Liong et al. 2002; Jakob et al. 2007; Xu and Tung 2009; Lee et al. 2010; Haddad et al. 2011; Dourte et al. 2013; Du et al. 2014; Khan et al. 2015 and Garcia-Urquia 2016).

Different approaches have been adopted for derivation of IFD curves. For example, Yu et al. (2004) developed IFD curves using data from 46 rain gauges over three regions in northern Taiwan. They pointed out that the IFD formula could be expressed in three ways depending on the types of scaling and the homogeneity of the regions. In another study, Nhat et al. (2006) derived IFD relationship for short durations based on daily rainfall data at two rainfall stations located at Yodo catchment in Japan. The new IFD curves showed better results as compared to IFD curves estimated by other methods such as Bernard equation (Bernard 1932). Overeem et al. (2008) adopted generalised least squares regression (GLSR) method and generalised extreme value (GEV) distribution to derive design rainfalls for 1–24-h durations using rainfall data from 12 stations in the Netherlands. The L-Moments method was adopted to calculate parameters of the GEV distribution. It was found that by using the bootstrap method, the uncertainties in design rainfalls could be estimated. Furthermore, it was noted that the shape parameter of the GEV distribution did not change with duration, while for the location parameter there was a notable increase as duration decreased.

Elsebaie (2011) developed IFD relationship for duration of 10–1440 min and return periods of 2–100 years for two stations at Najran and Hafr Albatin regions in the Kingdom of Saudi Arabia by using the Gumbel and the log Pearson type 3 distributions. A nonlinear regression analysis was adopted to estimate the parameters of IFD relationship at each region. The Chi-square test was used to select the best-fit statistical distribution. It was found that both the distributions produced similar IFD curves.

Mamoon et al. (2014) updated the IFD data in Qatar using L-Moments method and the index frequency method using daily rainfall data from 32 stations. It was found that the Pearson type 3 distribution provided the best fit to the daily duration annual maximum (AM) rainfall data. Liu et al. (2015) developed IFD curves using at-site and regional approaches as well as the corresponding confidence intervals at 9 rainfall stations in Jakarta area. The regional frequency analysis with L-Moments approach was used to analyse the AM rainfall series. With goodness-of-fit measure based on Monte Carlo simulation, GEV distribution was selected as the best-fit distribution. When comparing the quantiles of IFD curves and corresponding confidence intervals between at-site and regional approaches, it was found that the confidence intervals estimated by regional approach were generally smaller than those for the at-site approach.

In Australia, there have been a good number of studies on design rainfall estimation (e.g. Jakob et al. 2007; Haddad et al. 2010, 2011; Haddad and Rahman 2014; Yilmaz et al. 2014; Verdon-Kidd and Kiem 2015 and Bennett et al. 2016). For example, Jakob et al. (2007) applied L-Moments-based regionalisation method to the rainfall data in southeast Queensland and northeast New South Wales in Australia to IFD curves for durations of 24, 48 and 72 h and return periods of 1, 2, 5, 10, 20, 50 and 100 years. A partial least squares regression approach was used to derive reliable estimates of L-skewness and L-coefficient of variation to extend the study to the sub-daily durations of 1, 2, 3, 6 and 12 h. For selecting the best-fit distribution in the region, generalised logistic, GEV and generalised normal distributions were considered. The results showed that among the three-parameter distributions considered, the GEV gave the best fit. The validation against data in the pilot study area suggested good performance for 6- and 12-h durations. The comparison of the results of this study with those of Australian rainfall and runoff 1987 (ARR87) showed broad similarities in design rainfalls between the two methods.

Haddad et al. (2010) presented a statistical modelling framework to derive design rainfalls based on GLSR and L-Moments methods using data from 203 rainfall stations across Australia. By using the GLSR method, the regional prediction equations for the index rainfall, L-CV and L-skewness were developed for durations of 1–72 h. It was found that the proposed method, the GLSR coupled with L-Moments, was able to produce quite accurate design rainfall estimates for all the selected durations and return periods considered in the study. Also, it was found that a polynomial of third degree was sufficient for smoothing the IFD curves.

Haddad et al. (2011) developed IFD curves for short storm durations based on GLSR and L-Moments-based index methods using data from 203 rainfall stations across Australia. The Akaike and Bayesian information criteria were applied to identify a regional parent distribution. Monte Carlo simulation was adopted to estimate the sampling error variances of the AM series parameters (L-CV and L-skewness). The results showed that the GLSR performed relatively well for both the 6-min and 1-h durations. The generalised Pareto distribution appeared as the best-fit distribution. The new design rainfall estimates were generally greater than the at-site estimates, with some notable differences from the ARR87 estimates (I. E. Aust. 1987).

Haddad and Rahman (2014) developed a technique to derive short duration (sub-hourly and sub-daily durations) design rainfalls using long-duration rainfall statistics using L-Moments and GLSR to rainfall data set consisting of 203 rainfall stations. For estimating the design rainfall quantiles, the GEV distribution and generalised Pareto distribution were adopted. In another study, Haddad et al. (2015) compared three methods to form regions in rainfall frequency analysis using Australian data.

In Australia, the recommended IFD data are provided in Australian rainfall and runoff (ARR). The ARR1987 adopted LP3 distribution to derive IFD curves (I. E. Aust. 1987). In 2013, GEV distribution has been adopted to derive the IFD curves (Green et al. 2012; Ball et al. 2016) where a region of influence approach was adopted to form regions and a spline software was used to achieve spatial consistency in IFD data.

There have been many researches on design rainfall estimation as mentioned above. However, there is a lack of study on systematic comparison among IFD curves derived by different distributions and methods. It is important to assess how much variation in IFD values can occur when different probability distribution is adopted or between the IFD curves derived from at-site and regional frequency analyses. Hence, this research is devoted to compare IFD curves between a number of distributions and methods. In this paper, the following research questions are investigated. Firstly, how much variation in IFD curves is expected between two commonly adopted probability distributions, LP3 and GEV. Secondly, in smoothing the rainfall quantiles at a given site, whether empirical method or polynomial regression provides a better fitting. Finally, how the at-site IFD curves vary with the regional IFD curves. We use data from ten rainfall stations from NSW state in Australia to answer these research questions. We also use the regional IFD curves in Australia (from ARR 1987 and ARR 2016) to compare between the at-site and regional IFD curves (I. E. Aust. 1987; Ball et al. 2016). It is expected that the outcomes of this research will provide important guidance in validating the regional IFD curves, which are widely used in practice in preference to at-site IFD curves.

2 Study area and data

We use data from ten pluviograph stations from eastern New South Wales (NSW), Australia (Fig. 1). The rainfall data of each of these stations have been abstracted using HYDSTRA software from the database of Australian Bureau of Meteorology (BOM 2013). The rainfall data have record lengths greater than 30 years, ranging between 32 and 64 years with an average of 45 years (Table 1). The annual maximum (AM) rainfall events were extracted from rainfall records for each of the study stations. The AM rainfall events of these stations have less than 5% gaps. The primary rainfall data used in this study are recorded at 6-min interval; a FORTRAN program is developed to extract AM rainfall events of six sub-hourly durations (6, 12, 18, 24, 30 and 48 min), six sub-daily durations (1, 2, 3, 6, 8 and 12 h) and three daily durations (1, 2 and 3 days) for each of the ten rainfall stations.

3 Methods

In this study, stationary frequency analysis is applied to derive intensity frequency duration (IFD) curves at each of the selected stations for 7 return periods of 1, 2, 5, 10, 20, 50 and 100 years. The GEV and LP3 distributions are used to fit the rainfall intensity data for a

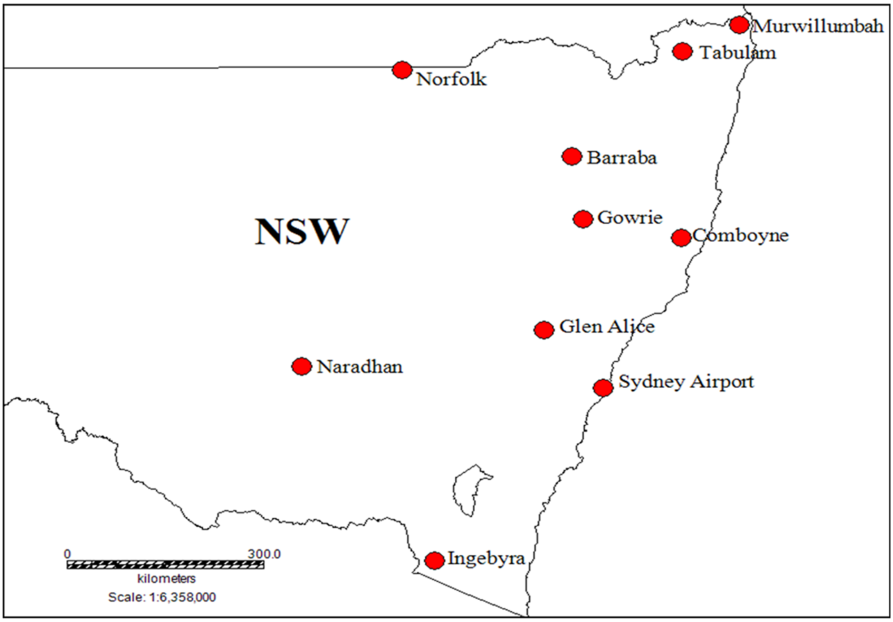

Fig. 1 Locations of the selected ten pluviograph stations in NSW, Australia

Table 1 Details of selected pluviography stations

Stations (name ID)	Period of rainfall record	Mean annual rainfall (mm)	Station elevation (m)	Latitude (°)	Longitude (°)
Barraba-054102	1972–2012	590	620	− 30.3735	150.6723
Gowrie-055194	1972–2012	570	518	− 31.3365	150.8537
Tabulam-057095	1970–2012	879	555	− 28.7551	152.4507
Murwillumbah-058158	1973–2012	1384	8	− 28.3395	153.3809
Comboyne-060080	1967–2012	1481	670	− 31.6274	152.443
Glen Alice-061334	1971–2012	380	320	− 33.0488	150.2325
Sydney Airport-066037	1963–2012	917	6	− 33.9465	151.1731
Ingebyra-071042	1972–2012	577	1215	− 36.6022	148.4677
Naradhan-075050	1971–2012	301	192	− 33.6104	146.3161
Norfolk-200288	1949–2012	1002	111.7	− 29.0389	147.9408

given duration at a given station. The reason for using these two distributions is that they have been used widely in rainfall frequency analysis in previous studies (e.g. Nhat et al. 2006; Elsebaie 2011; Haddad and Rahman 2014; Liu et al. 2015; Ball et al. 2016). Three goodness-of-fit tests (i.e. Kolmogorov–Smirnov, Anderson–Darling and Chi-square tests) are adopted to assess the goodness-of-fit of the GEV and LP3 distributions. To establish the relationship between the estimated rainfall quantiles, rainfall duration and return period, two methods have been adopted (empirical and polynomial). A brief description of each of these statistical techniques is presented below.

3.1 Generalised extreme value (GEV) distribution

GEV distribution is a continuous probability distribution developed within extreme value theory to combine the Fréchet (1927), Weibull (1951) and Gumbel (1958) families of distributions. The GEV distribution has three parameters (location: ξ; scale: α; and shape: κ), and it is used as an approximation to model the maxima of long sequences of random variables. The GEV distribution is equivalent to a Gumbel, Fréchet or Weibull distribution depending on whether $\kappa = 0$, $\kappa > 0$ or $\kappa < 0$, respectively. The GEV distribution has the cumulative density function (CDF) and probability density function (PDF) (Hosking and Wallis 1997) as shown below:

$$F(x;\zeta,\alpha,\kappa) = \exp\left\{-\left(1+\frac{\kappa(x-\xi)}{\alpha}\right)^{-1/\kappa}\right\} \tag{1}$$

$$f(x;\zeta,\alpha,\kappa) = \alpha^{-1}\exp\left\{\left(\frac{1}{\kappa}+1\right)\times\log\left(1-\frac{\kappa(x-\xi)}{\alpha}\right)-\exp\left(-\frac{(x-\xi)}{\alpha}\right)\right\} \tag{2}$$

where x refers to the primary data series which is to be fitted by the GEV distribution.

3.2 Log Pearson type 3 distribution (LP3)

The LP3 distribution is a three-parameter distribution (similar to GEV), and it uses location (μ), scale (σ) and shape (γ) parameters (Millington et al. 2011).

To calculate the T-year event quantile, the LP3 distribution based on the mean (μ), standard deviation (σ) and skewness (γ) becomes:

$$Q_{\mathrm{T}} = \mu + K_{\mathrm{T}}\sigma \tag{3}$$

where K_{T} is frequency factor for return period T, which depends on skewness.

3.3 L-Moments method

In this study, L-Moments method is used to fit the GEV distribution. L-Moments are defined as liner combinations of probability weighted moments (PWMs), which were introduced by Greenwood et al. (1979) and others (i.e. Landwehr et al. 1979; Wallis 1980; Greis and Wood 1983; Hosking et al. 1985; Hosking and Wallis 1987) to develop statistical inference procedures for use as a tool for estimating the parameters of probability distributions.

3.4 Goodness-of-fit tests

In this study, three goodness-of-fit tests are used to assess how well a given distribution fits the rainfall data series of a given duration. The detail of each test is provided below:

3.5 Kolmogorov–Smirnov test

The Kolmogorov–Smirnov (KS) test (Kirkman 1996) utilises the greatest vertical difference between the theoretical and the empirical cumulative distribution functions:

$$KS = \max_{1 \le i \le n}\left\{F(X_i) - \frac{i-1}{n}, \frac{i}{n} - F(X_i)\right\} \tag{4}$$

3.6 Anderson–Darling test

Anderson–Darling (AD) test (Scholz and Stephens 1987) gives more weight to the tails of the distribution and is defined by the following equation:

$$AD^2 = -n - \frac{1}{n}\sum_{i=1}^{n}(2i-1)[\ln(F(X_i) + \ln(1 - F(X_{n-i+1})))] \tag{5}$$

3.7 Chi-square test

The Chi-square (χ^2) test (Preacher 2001) is applied to binned data. The χ^2 test statistic is defined as:

$$\chi^2 = \sum_{i=1}^{N}(O_i - E_i)^2/E_i \tag{6}$$

where O_i is the observed frequency of the data sample and E_i is the expected frequency of data sample calculated by $E_i = F(X_2) - F(X_1)$, where F is the cumulative distribution function of the probability distribution being tested.

The test is conducted at three significance levels (10, 5 and 1%).

3.8 Developing IFD curves

Once the seven rainfall quantiles (T = 1, 2, 5, 10, 20, 50 and 100 years) are estimated from the fitted GEV (or LP3) distribution, the IFD curve is developed in two ways: (1) making an empirical relationship among rainfall intensity (I), duration (D) and return period (T); and (2) fitting a second-degree polynomial among the seven I values. The empirical relationship is expressed mathematically as follows:

$$I = F(T, D) \tag{7}$$

The empirical IFD relationship is given by the below equation:

$$I = f \times T/(D^v + l)^e \tag{8}$$

where I refers to a rainfall intensity (mm/hr), T is return period (year), D is duration (minutes), and f, l, e and v are coefficients.

The adopted polynomial equation has the following form:

$$log\,(I_\mathrm{T}) \;=\; a \times (log\,(D))^2 + b \times log\,(D) \;+\; c \tag{9}$$

where a, b, c are constants estimated by polynomial regression analysis using XLSTAT software.

3.9 Relative error and root mean square error

In this study, the relative accuracy of the new IFD curves is assessed by calculating the relative error (RE) and the root mean square error (RMSE) (expressed by Eqs. 10 and 11) between the new IFD values (I_{new}) and the IFD values recommended in Australia for general use, i.e. ARR87 and ARR13 IFD values (I_{ARR}) (I. E. Aust. 1987 and Ball et al. 2016).

$$\mathrm{RE}(\%) = \left(\frac{I_{\mathrm{new}} - I_{\mathrm{ARR}}}{I_{\mathrm{new}}}\right) \times 100 \tag{10}$$

$$\mathrm{RMSE}(\%) = \sqrt{\frac{1}{n}\sum_{i=1}^{n}\left(\frac{I_{\mathrm{new}} - I_{\mathrm{ARR}}}{I_{\mathrm{new}}}\right)^2} \times 100 \tag{11}$$

4 Results

4.1 Goodness-of-fit tests

Three goodness-of-fit tests (i.e. KS, AD and χ^2) (described in Sect. 3) were used in this study to choose the better statistical distribution among the two adopted distributions (GEV and LP3). Depending on the AM rainfall data series of the ten selected stations and 15 rainfall durations, a total of 150 data sets (i.e. 10 $\times$ 15) were available for the goodness-of-fit testing. Depending on the results of goodness-of-fit tests, GEV and LP3 distributions showed a minor difference in fitting the AM rainfall data series. At the three significance levels (10, 5 and 1%) and out of the 150 data sets (Table 2), the KS and AD tests did not reject GEV distribution in any of the cases, while Chi-square test rejected GEV just one occasion (for rainfall data series of 120 min duration at station Barraba- 054102). The KS

Table 2 Number of rejections (out of 150 cases) at the three significance levels (10, 5 and 1%) for the *KS*, *AD* and Chi-square goodness-of-fit tests

Distribution	GEV			LP3		
Significance level	10%	5%	1%	10%	5%	1%
KS	0	0	0	0	0	0
AD	0	0	0	1	1	1
χ^2	1	1	1	0	0	0

test also did not reject the LP3 distribution for any of the cases. The *AD* test rejected the LP3 distribution just one occasion (for rainfall data series of 6 min duration at station Murwillumbah-058158). Finally, the Chi-square test did not reject LP3 in any cases.

4.2 Shape parameter for the GEV distribution

In estimating extreme rainfall, tail of the distribution is of special significance, which is governed by the shape parameter. As noted in Sect. 3, the GEV distribution belongs to one of the three families of extreme value distributions (i.e. Gumbel, Fréchet and Weibull families) depending on the value of shape parameter (i.e. if it is 0, larger than 0 or less than 0). Therefore, it is of importance to test whether the shape parameter equals to 0 or not.

In this section, the results of the shape parameter of the GEV distribution for the AM rainfall data at the ten rainfall stations are examined. Figure 2 shows the boxplot of the shape parameter values. For 6-min duration, the shape parameter is generally negative, with a median value of − 0.083, while for 4320-min (3 days) duration, the shape parameter is dominated by positive values, with a median value of 0.036. For the sub-hourly durations, most of the stations are dominated by negative shape parameters, and for the sub-daily and daily durations, the shape parameters are generally positive. For the 1 h, the shape parameter has a median very close to 0. Among the ten stations, the minimum value of the shape parameter is − 0.319 (for 6 min rainfall duration), and the maximum value is 0.288 (for 12 h rainfall duration). The regional average (over the ten stations)

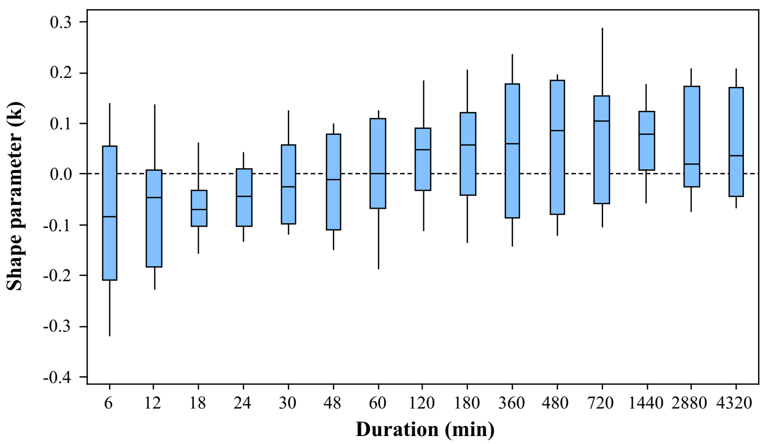

Fig. 2 Boxplots of shape parameters of the GEV distribution at ten stations in NSW

Table 3 Quartile information of the shape parameter of the GEV distribution for ten stations in NSW

Duration (min)	Quartile 1	Quartile 2 (median)	Quartile 3	Min	Max
6	− 0.209	− 0.083	0.056	− 0.319	0.140
12	− 0.183	− 0.047	0.009	− 0.228	0.139
18	− 0.103	− 0.071	− 0.031	− 0.158	0.063
24	− 0.103	− 0.045	0.011	− 0.134	0.044
30	− 0.098	− 0.025	0.057	− 0.120	0.125
48	− 0.109	− 0.010	0.079	− 0.149	0.099
60	− 0.068	0.000	0.110	− 0.188	0.126
120	− 0.033	0.048	0.090	− 0.112	0.186
180	− 0.042	0.057	0.121	− 0.136	0.206
360	− 0.085	0.059	0.178	− 0.144	0.238
480	− 0.079	0.086	0.185	− 0.122	0.198
720	− 0.057	0.105	0.154	− 0.105	0.288
1440	0.009	0.078	0.124	− 0.058	0.177
2880	− 0.026	0.019	0.173	− 0.075	0.208
4320	− 0.043	0.036	0.171	− 0.067	0.209

value of the shape parameters is 0.011, with 79 positive values and 71 negative values. All the five important quartile values of the shape parameters are presented in Table 3.

4.3 Development of the IFD curves

The empirical relationship of the IFD curves based on Eq. 8 for each of the ten stations is presented in Table 4 (where 7 basic quantiles were estimated using fitted GEV distribution) and Table 5 (quantiles estimated by LP3 distribution). The coefficient of determination (R^2) values of the fitted empirical IFD curves range 0.981–0.995 (average = 0.990) for the GEV case. For the LP3 distribution, R^2 values range 0.977–0.996 (average = 0.988). These show that the R^2 values are quite high for the empirical IFD curves.

Table 4 Empirical relationship between I (mm/hr) (estimated by GEV distribution), T (years) and D (min) at the ten selected stations

Stations (name ID)	Relationship	R^2	RMSE (%)
Barraba-054102	$I = 799.855 \times (T^{0.225})/(12.397 + D)^{0.801}$	0.990	4.849
Gowrie-055194	$I = 397.363 \times (T^{0.261})/(3.848 + D)^{0.747}$	0.995	3.315
Tabulam-057095	$I = 1979.797 \times (T^{0.204})/(23.513 + D)^{0.953}$	0.991	4.535
Murwillumbah-058158	$I = 355.509 \times (T^{0.221})/(2.115 + D)^{0.561}$	0.992	5.732
Comboyne-060080	$I = 233.344 \times (T^{0.209})/(0.234 + D)^{0.522}$	0.991	4.482
Glen Alice-061334	$I = 616.606 \times (T^{0.190})/(7.256 + D)^{0.808}$	0.994	3.153
Sydney Airport-066037	$I = 794.817 \times (T^{0.224})/(20.908 + D)^{0.727}$	0.992	4.259
Ingebyra-071042	$I = 196.737 \times (T^{0.278})/(2.700 + D)^{0.635}$	0.991	3.355
Naradhan-075050	$I = 1327.614 \times (T^{0.199})/(15.497 + D)^{0.995}$	0.985	4.340
Norfolk-200288	$I = 206.215 \times (T^{0.318})/(-2.088 + D)^{0.555}$	0.981	6.205
AVG. ± SD		0.990 ± 0.004	4.423 ± 0.954

Table 5 Empirical relationship between I (mm/hr) (estimated by the LP3 distribution), T (years) and D (min) (estimated by LP3) at the ten selected stations

Stations (name ID)	Relationship	R^2	RMSE (%)
Barraba-054102	$I = 887.463 \times (T^{0.176})/(12.884 + D)^{0.790}$	0.991	4.338
Gowrie-055194	$I = 521.980 \times (T^{0.200})/(3.918 + D)^{0.778}$	0.988	5.021
Tabulam-057095	$I = 2959.644 \times (T^{0.144})/(28.841 + D)^{0.992}$	0.989	4.617
Murwillumbah-058158	$I = 389.330 \times (T^{0.161})/(1.570 + D)^{0.549}$	0.990	5.854
Comboyne-060080	$I = 250.018 \times (T^{0.163})/(-0.578 + D)^{0.518}$	0.986	5.357
Glen Alice-061334	$I = 665.172 \times (T^{0.127})/(6.969 + D)^{0.794}$	0.996	2.468
Sydney Airport-066037	$I = 1043.454 \times (T^{0.187})/(21.689 + D)^{0.765}$	0.993	4.096
Ingebyra-071042	$I = 177.687 \times (T^{0.224})/(0.410 + D)^{0.575}$	0.985	4.251
Naradhan-075050	$I = 2140.578 \times (T^{0.149})/(19.043 + D)^{1.064}$	0.988	3.792
Norfolk-200288	$I = 253.819 \times (T^{0.262})/(-2.459 + D)^{0.563}$	0.977	6.430
AVG. ± SD		0.988 ± 0.005	4.622 ± 1.063

The *RMSE* values (estimated by Eq. 11) range 3.153 and 6.205% (average = 4.423) for the GEV distribution, while for LP3 distribution range 2.468 and 6.430% (average = 4.622). These results imply that confidence can be placed on the empirical equations used to derive IFD curves.

The complete set of IFD curves obtained by the fitted empirical equations (shown in Tables 4 and 5) for the three stations (Gowrie-055194, Comboyne-060080 and Ingebyra-071042) are presented in Figs. 3 and 4 as examples. These figures show that there is a high degree of consistency in the developed IFD curves across different return periods. Also, these figures show that the IFD curves have a negative gradient, consistent with experience that higher rainfall intensity occurs over shorter durations.

The second-degree polynomial was used to derive the relationship of an IFD curve based on Eq. 9 for each of the ten stations. Table 6 shows the R^2 values of the fitted second-degree polynomial IFD curves for all the 7 return periods. The R^2 values range 0.997–0.999 (average = 0.998). Also, it can be seen that the RMSE values range 1.015 to 3.851% for the GEV distribution case, and 1.113–3.607% for LP3 distribution case. The R^2 values for the second-degree polynomial are found to be higher than those obtained by using the empirical method (Tables 4 and 5); therefore, it can be concluded that the second-degree polynomial has resulted in more accurate IFD curves than the empirical method. As examples, Figs. 5, 6, 7 and 8 show the IFD curves derived by the second-

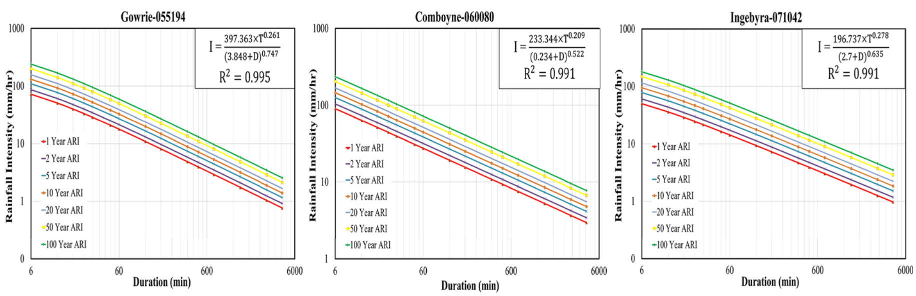

Fig. 3 Examples of developed IFD curves based on empirical relationships shown in Table 5 (GEV distribution case)

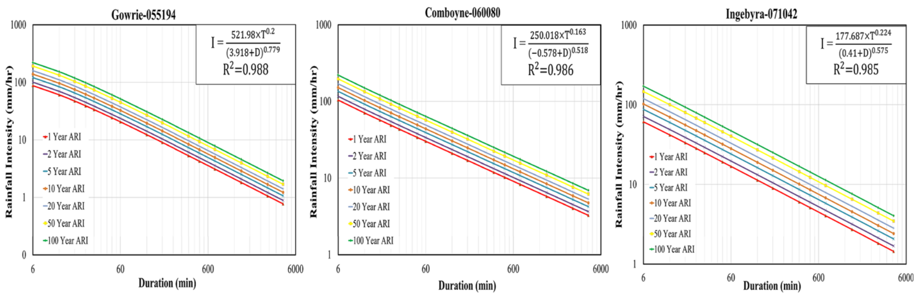

Fig. 4 Examples of developed IFD curves based on empirical relationships shown in Table 6 (LP3 distribution case)

Table 6 Average coefficient of determination (R^2) and RMSE values for all the ten stations (case of the fitted second-degree polynomial IFD curves)

Distribution	GEV		LP3	
Return period (year)	AVG. ($R^2 \pm$ SD)	AVG. (RMSE $\pm$ SD)	AVG. ($R^2 \pm$ SD)	AVG. (RMSE $\pm$ SD)
1	0.998 ± 0.001	1.015 ± 0.463	0.998 ± 0.002	1.113 ± 0.632
2	0.998 ± 0.002	1.073 ± 0.564	0.998 ± 0.001	1.099 ± 0.624
5	0.999 ± 0.001	1.251 ± 0.683	0.999 ± 0.001	1.404 ± 0.619
10	0.999 ± 0.001	1.405 ± 0.738	0.998 ± 0.001	1.835 ± 0.732
20	0.999 ± 0.001	1.744 ± 0.814	0.998 ± 0.002	2.340 ± 0.892
50	0.998 ± 0.001	2.704 ± 0.973	0.997 ± 0.002	3.056 ± 1.140
100	0.997 ± 0.002	3.851 ± 1.197	0.997 ± 0.003	3.607 ± 1.352

degree polynomial for the three rainfall stations (i.e. Gowrie-055194, Comboyne-060080 and Ingebyra-071042) and two return periods (5 and 100 years).

4.4 Visualisation of derived IFD curves with respect to observed AM rainfall data

Figures 9 and 10 show the new IFD curves (by the empirical and polynomial fitting methods) along with the observed AM rainfall data for the same three stations as above

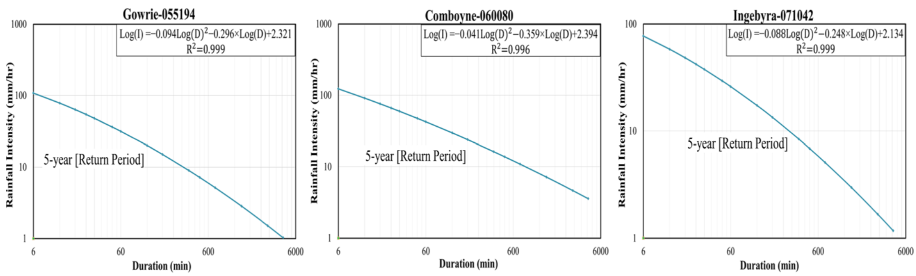

Fig. 5 Fitting a second-degree polynomial between I and D estimated by GEV distribution for 5-year return period

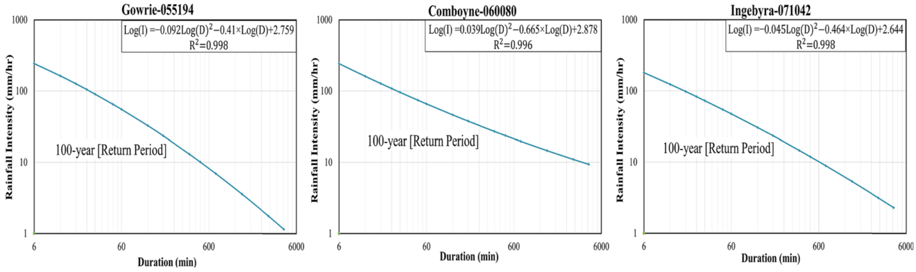

Fig. 6 Fitting a second-degree polynomial between *I* and *D* estimated by GEV distribution for 100-year return period

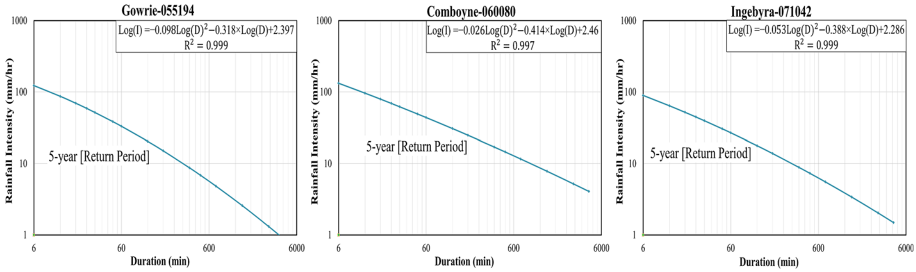

Fig. 7 Fitting a second-degree polynomial between *I* and *D* estimated by LP3 distribution for 5-year return period

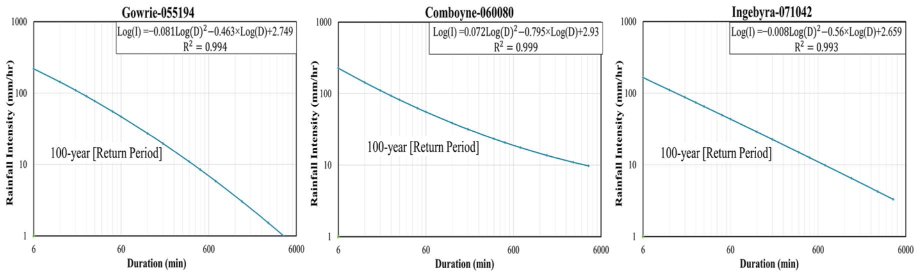

Fig. 8 Fitting a second-degree polynomial between *I* and *D* estimated by LP3 distribution for 100-year return period

(Gowrie-055194, Comboyne-060080 and Ingebyra-071042). Weibull plotting position formula was used to plot the AM rainfall data. These two figures show that the IFD curves obtained from second-degree polynomial (IFD*: red colour) generally match the AM rainfall data more closely than IFD curves obtained from the empirical relationship (IFD**: blue colour). Moreover, it is noted that in general for shorter rainfall durations such as 6 min, the IFD curves better fit the AM rainfall data than those of longer durations such 180 and 2880 min.

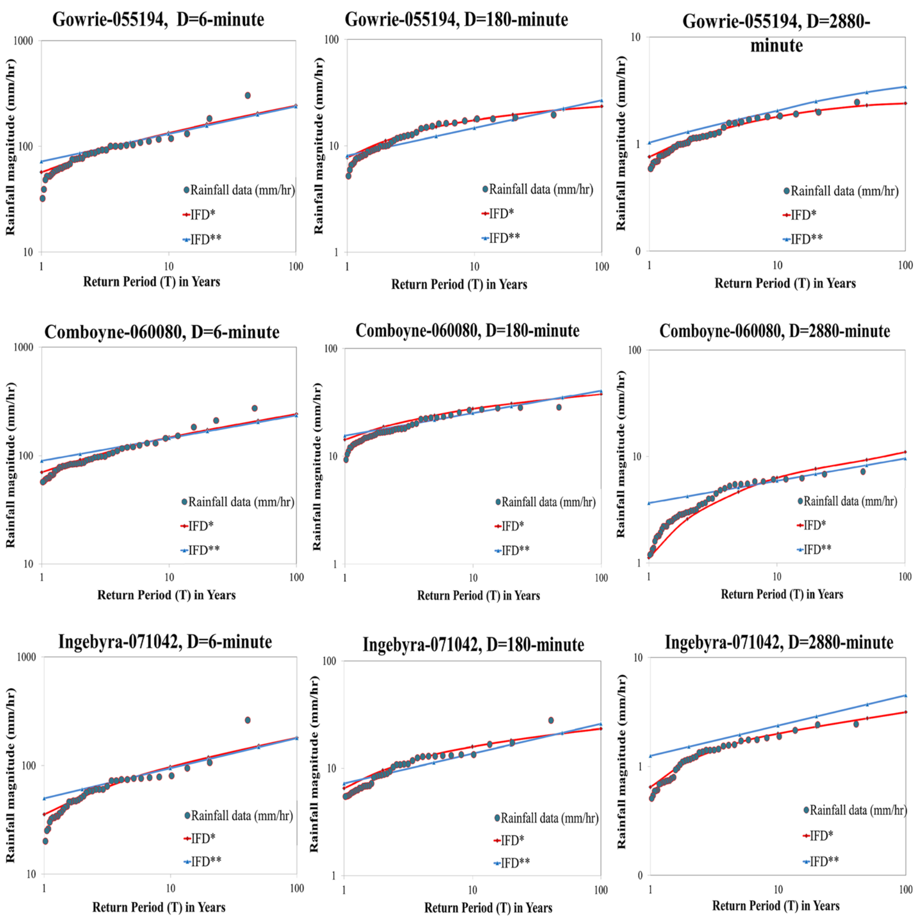

Fig. 9 IFD curves from polynomial equations (IFD*) and IFD curves from empirical formula (IFD**): GEV distribution case

4.5 Comparison of estimated IFD curves with the ARR87 and ARR13

The new IFD curves based on both the adopted distributions (GEV and LP3) were compared with IFD curves recommended by ARR87 (I. E. Aust. 1987) and ARR13 (Ball et al. 2016). The comparison is illustrated for two return periods (5 and 100 years) for three stations (i.e. Gowrie-055194, Comboyne-060080 and Ingebyra-071042) in Fig. 11. This figure shows that for the three selected stations, there are quite good match between the new IFD curves (based on GEV distribution) and ARR13 IFD curves. Also, our new IFD curves (based on LP3 distribution) exhibit a quite good match with those of the ARR87. Also, this figure shows that for 100-year return period, the IFD curves have slightly more kinks especially for longer durations (i.e. greater than 60 min), which is not unexpected.

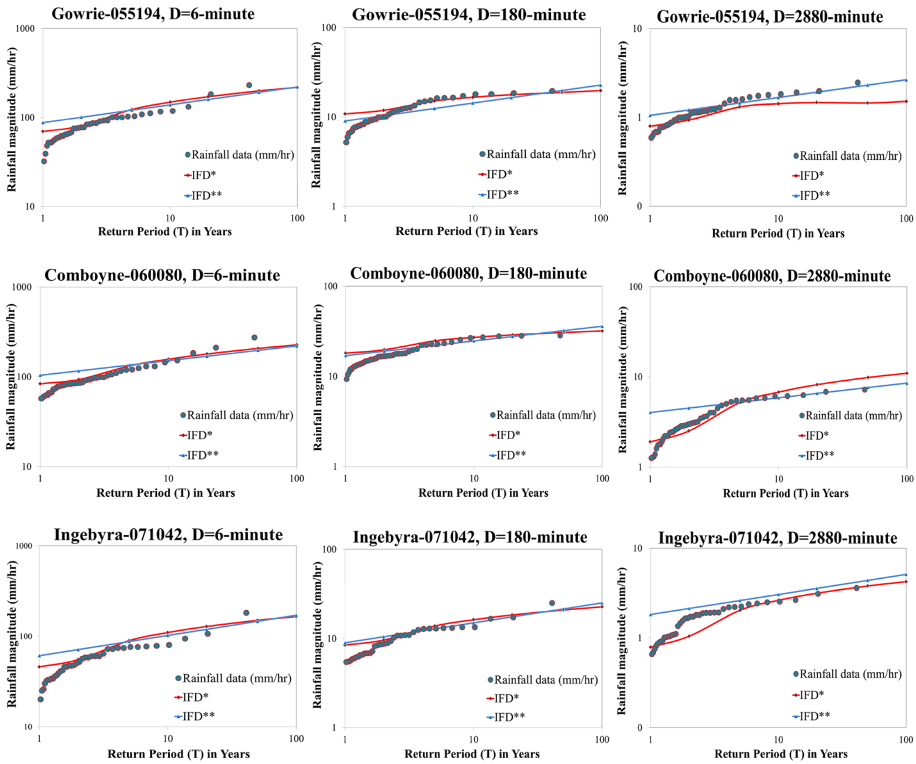

Fig. 10 IFD curves from polynomial equations (IFD*) and IFD curves from empirical formula (IFD**): LP3 distribution case

For evaluating the accuracy of the new IFD curves, the relative error (RE) (defined by Eq. 10) and root mean square error values (RMSE) (defined by Eq. 11) were used. Table 7 shows the absolute median RE values (%) between the new IFD curves and the ARR IFD curves (i.e. ARR87 and ARR13), which shows that the absolute median RE values range between 1 and 48% for the ten selected stations, with a mean RE value of 14.73%, and with a standard deviation of RE values of 9.93% (based on GEV distribution) and with a mean RE value of 17.20%, and with a standard deviation of RE values of 11.97% (based on LP3 distribution). As the return period increases, the absolute RE values generally increase. For stations Norfolk-200288, the RE values are the largest, and for station Glen Alice-061334, the RE values are quite high for the ARR87 case. Overall, considering all the seven return periods and ten stations, the average median RE value is the smallest (5.3%) between the new IFD curves (based on the GEV distribution) and the ARR13 IFD curves. Furthermore, the average highest median RE value (37.3%) is found between the new IFD curves (based on LP3 distribution) and ARR87 IFD curves. It should be noted here that the ARR87 and ARR13 IFD curves were not at-site IFD curves (they were regional IFD curves that were also subjected to regional smoothing), and hence, some differences between ARR and our new IFD curves are expected.

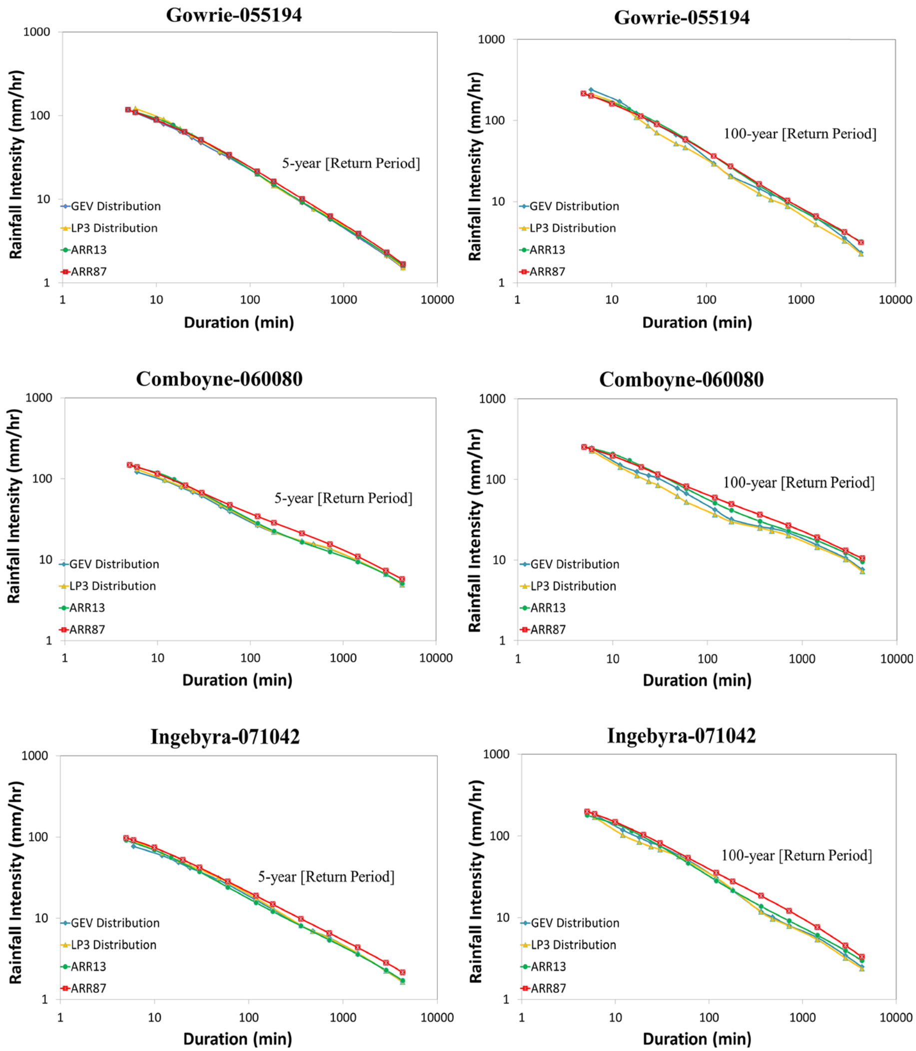

Fig. 11 Comparison of at-site IFD curves with ARR13 and ARR87 IFD curves for 5- and 100-year return periods

The boxplots of the RE values (considering the sign of RE) were examined. (An example is shown in Fig. 12 for station Gowrie-055194.) These boxplots show that the new IFD values are generally smaller than the ARR87 and ARR13 IFD curves.

Figure 13 shows the spatial distribution of median RE values (%) (considering sign) between the new IFD curves and the ARR IFD curves (ARR87 and ARR13) for 5-year return period. From Fig. 13, it can be seen that for 5-years return period, the RE values are generally negative, i.e. the new IFD curves are smaller than the ARR IFD curves. However, the new IFD curves based on GEV distribution (Fig. 13b) show the lowest

Table 7 Absolute median relative error (RE) values (%) between the new IFD curves and ARR87 and ARR13 IFD curves

Stations	Dist.	GEV								LP3							
	T (year)	1	2	5	10	20	50	100	AVG.	1	2	5	10	20	50	100	AVG.
Barraba-054102	ARR87	4	20	10	9	10	12	16	11.6	5	15	10	9	9	17	23	12.6
	ARR13	7	7	10	10	10	13	14	10.1	3	4	8	12	11	12	9	8.4
Gowrie-055194	ARR87	5	17	10	6	9	13	16	10.9	4	12	8	7	12	20	27	12.9
	ARR13	9	5	4	4	8	9	9	6.9	2	1	3	5	12	20	27	10.0
Tabulam-057095	ARR87	5	13	7	6	8	9	10	8.3	8	7	6	8	11	16	20	10.9
	ARR13	3	3	5	11	18	25	29	13.4	5	4	6	12	20	30	39	16.6
Murwillumbah-058158	ARR87	8	18	12	11	15	21	26	15.9	6	11	11	12	20	31	39	18.6
	ARR13	18	7	5	4	7	12	18	10.1	14	11	4	6	15	30	41	17.3
Comboyne-060080	ARR87	3	24	17	14	18	21	24	17.3	5	20	14	16	22	32	41	21.4
	ARR13	8	2	4	7	11	13	16	8.7	8	4	4	9	15	24	31	13.6
Glen Alice-061334	ARR87	14	42	35	28	27	25	23	27.7	23	36	28	25	29	31	36	29.7
	ARR13	10	13	13	12	13	17	20	14.0	14	9	8	11	20	28	36	18.0
Sydney Airport-066037	ARR87	6	19	11	6	5	4	6	8.1	5	12	6	5	10	17	22	11.0
	ARR13	8	7	9	8	10	13	17	10.3	9	12	10	12	15	15	20	13.3
Ingebyra-071042	ARR87	8	22	16	14	18	25	31	19.1	5	21	14	13	18	27	33	18.7
	ARR13	7	3	4	3	5	8	8	5.4	4	3	4	5	7	10	13	6.6
Naradhan-075050	ARR87	12	12	8	7	11	19	26	13.6	7	9	7	8	15	26	34	15.1
	ARR13	2	4	8	12	17	25	30	14.0	3	4	6	14	22	33	43	17.9
Norfolk-200288	ARR87	30	34	35	37	37	39	38	35.7	48	38	40	41	37	31	26	37.3
	ARR13	27	40	36	35	35	32	29	33.4	46	44	41	38	32	23	16	34.3
ARR87(AVG. ± SD)									16.8 ± 8.8								18.8 ± 8.7
ARR13(AVG. ± SD)									12.6 ± 7.9								15.6 ± 7.7

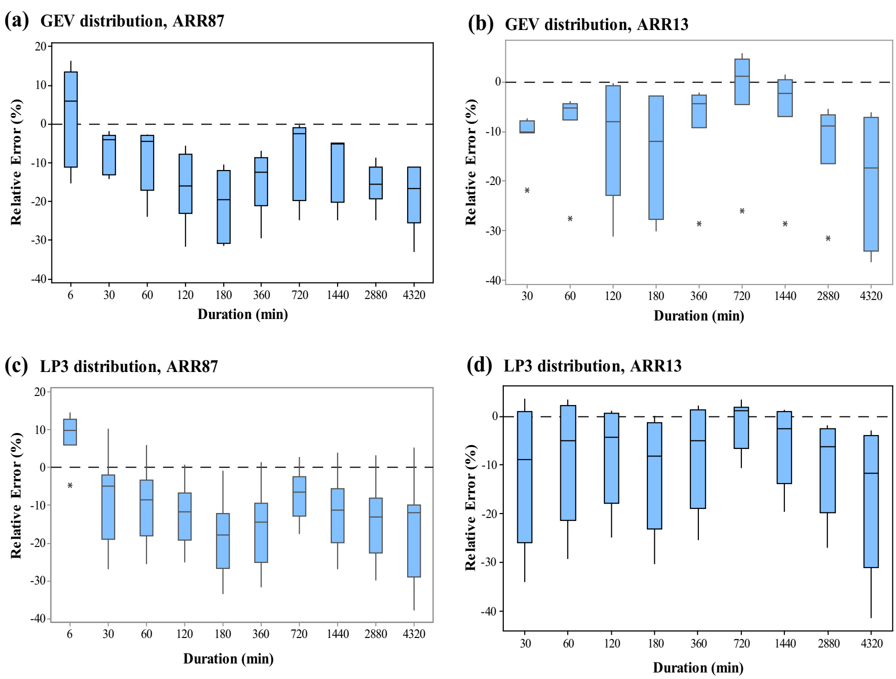

Fig. 12 Boxplots for relative error (RE) (considering sign of RE) for the 7 return periods and for the station Gowrie-055194. **a** RE estimated between the new IFD curves based on GEV distribution and ARR87. **b** RE estimated between the new IFD curves based on GEV distribution and ARR13. **c** RE estimated between the new IFD curves based on LP3 distribution and ARR87. **d** RE estimated between the new IFD curves based on LP3 distribution and ARR13

degree of differences (with 5 positive RE and 5 negative RE values out of ten stations) with the ARR13 IFD curves. Figure 14 shows the spatial distribution of median RE values (%) (considering sign) between the new IFD curves and the ARR IFD curves (ARR87 and ARR13) for 100 years return period. It can be seen from Fig. 14 that the new IFD curves are smaller than the ARR IFD curves for majority of the selected ten stations.

Table 8 summarises root mean square error (RMSE) values (estimated by Eq. 11) for all the seven return periods and ten selected stations. Overall, considering all the return periods and stations, the median RMSE value is the smallest (14.0%) between the new IFD curves (based on the GEV distribution) and the ARR13 IFD curves. Furthermore, the highest median RMSE value (20.6%) is found between the new IFD curves (based on LP3 distribution) and ARR87 IFD curves. Moreover, it can be seen that the lowest RMSE value is 6.3% for station Ingebyra-071042 (based on GEV distribution), while the highest RMSE value is 45% for station Murwillumbah-058158 (based on LP3 distribution).

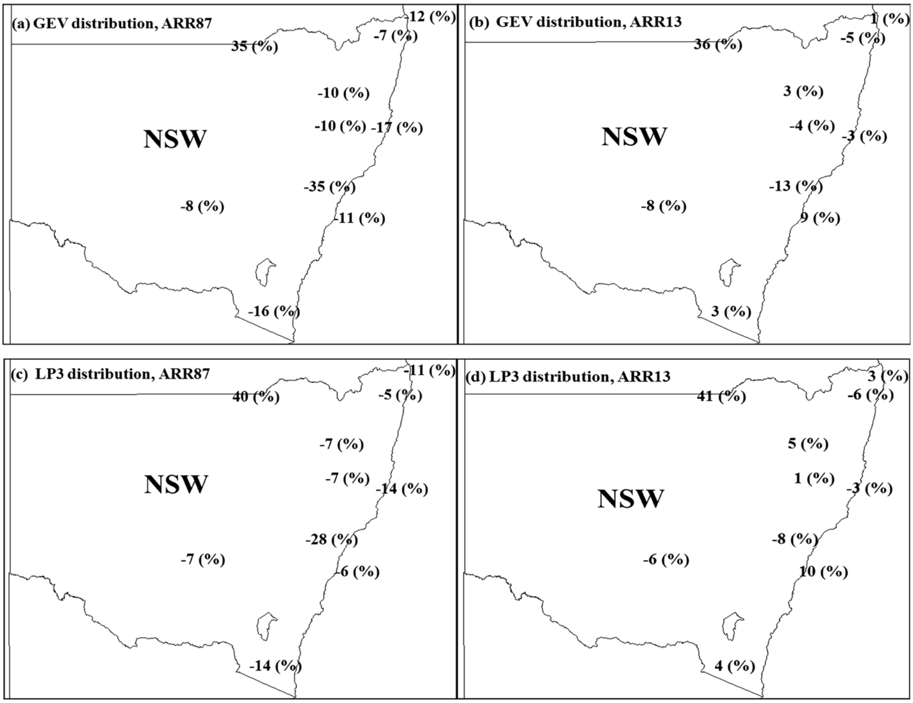

Fig. 13 Distribution of median RE values (%) between the new IFD curves based on GEV distribution and the **a** ARR87, **b** ARR13 and the new IFD curves based on the LP3 distribution and **c** ARR87 and **d** ARR13 IFD curves (5-year return periods)

5 Conclusions

The intensity–frequency–duration (IFD) data, also known as design rainfall, are widely used in planning, designing and operation of water resources management projects. The reviewing/updating of IFD curves is an important research task in hydrology. This study compares the latest regional IFD curves in Australia, published in 2013, as a part of the new Australian rainfall and runoff (ARR) 2016 (Ball et al. 2016) with the at-site IFD curves to examine the expected degree of variation between the at-site and regional IFD data. It uses data from ten pluviography stations from eastern New South Wales (NSW), Australia. Fifteen rainfall durations (6 min to 3 days) and seven return periods (i.e. 1, 2, 5, 10, 25, 50 and 100 years) are considered. The IFD curves generated by two commonly used probability distributions, generalised extreme value (GEV) and log Pearson type 3 (LP3) distributions are compared. Empirical and polynomial regression methods are used for smoothing the IFD curves at a given site. Based on the three goodness-of-fit tests (i.e. Kolmogorov–Smirnov test, Anderson–Darling test and Chi-square test), it has been found

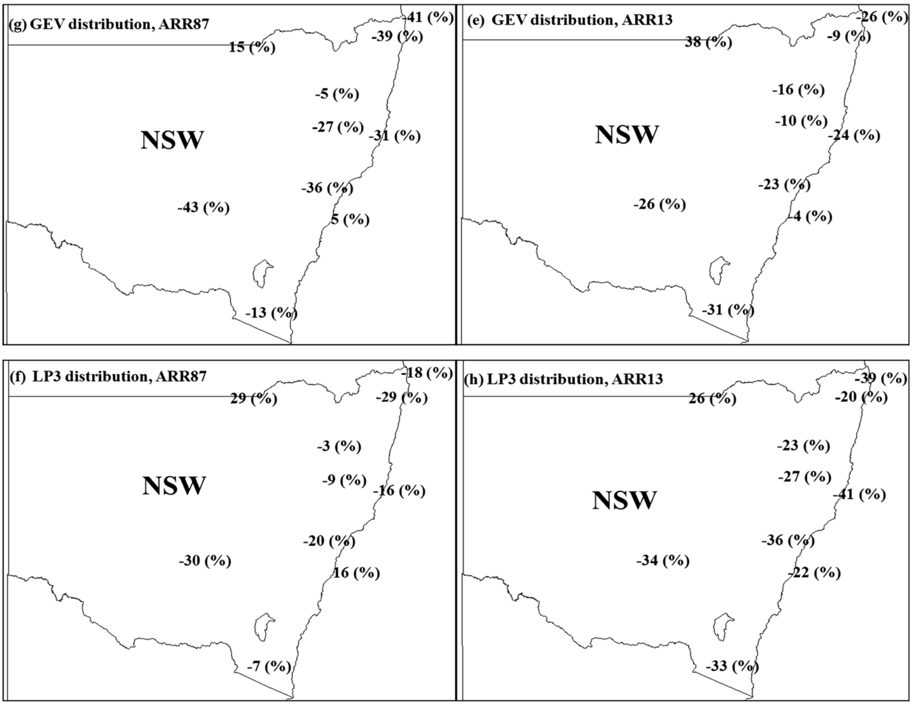

Fig. 14 Distribution of median RE values (%) between the new IFD curves based on GEV distribution and the **e** ARR87, **f** ARR13 and the new IFD curves based on the LP3 distribution and **g** ARR87 and **h** ARR13 IFD curves (100-year return periods)

that both GEV and LP3 distributions fit the annual maximum rainfall data (at 1% significance level) for all the ten selected stations. The developed IFD curves based on the second-degree polynomial represent better fitting than the empirical method. It has been found that the ARR87 and ARR13 IFD curves are generally higher than the at-site IFD curves derived here. The median difference between the at-site and regional ARR-recommended IFD curves is in the range of 13–19%. It is expected that the outcomes of this research will provide better guidance in selecting the correct IFD data for a given application in eastern NSW. The methodology developed here should be extended to more rainfall stations across Australia to have a better understanding of the possible differences in IFD data between different distributions and at-site and regional analyses.

Table 8 Root mean square error (RMSE) values (%) between the quantiles of the GEV and LP3 distributions and the quantiles of ARR87 and ARR13 for each of the ten selected stations

Stations	Dist.	GEV								LP3							
	T (year)	1	2	5	10	20	50	100	AVG.	1	2	5	10	20	50	100	AVG.
Barraba-054102	ARR87	7	19	12	10	12	16	20	13.7	8	16	11	11	15	22	28	15.9
	ARR13	8	7	9	11	12	15	18	11.4	6	7	11	12	15	21	27	14.1
Gowrie-055194	ARR87	11	17	10	7	10	15	19	12.7	5	12	8	9	13	21	27	13.6
	ARR13	9	5	5	6	9	14	19	9.6	2	2	3	7	12	21	28	10.7
Tabulam-057095	ARR87	6	15	8	7	10	14	18	11.1	10	12	8	9	13	20	27	14.1
	ARR13	5	10	10	13	16	21	26	14.4	6	6	8	13	18	28	36	16.4
Murwillumbah-058158	ARR87	4	21	15	12	16	21	26	16.4	7	14	12	14	23	35	45	21.4
	ARR13	8	7	4	5	8	15	21	9.7	12	10	4	7	15	28	38	16.3
Comboyne-060080	ARR87	11	24	20	19	22	28	32	22.3	8	20	18	19	27	36	44	24.6
	ARR13	8	3	6	8	10	15	19	9.9	7	5	4	8	14	24	32	13.4
Glen Alice-061334	ARR87	27	49	36	28	27	25	24	30.9	31	44	30	26	29	34	39	33.3
	ARR13	12	20	18	18	19	20	21	18.3	17	16	13	16	20	28	34	20.6
Sydney Airport-066037	ARR87	3	21	14	10	11	12	13	12.0	7	15	10	9	13	19	24	13.9
	ARR13	20	8	12	13	15	17	19	14.9	11	11	15	15	15	18	22	15.3
Ingebyra-071042	ARR87	15	31	19	16	19	26	32	22.6	14	27	17	16	21	29	36	22.9
	ARR13	3	4	5	5	6	9	12	6.3	4	4	7	7	8	12	15	8.1
Naradhan-075050	ARR87	18	14	13	13	18	25	31	18.9	10	10	12	15	23	35	45	21.4
	ARR13	6	5	8	12	17	24	30	14.6	8	5	7	14	22	33	42	18.7
Norfolk-200288	ARR87	29	33	35	36	35	34	34	33.7	45	36	39	38	35	29	26	35.4
	ARR13	27	38	35	32	31	29	28	31.4	44	41	37	33	29	23	19	32.3
ARR87(AVG. ± SD)									19.4 ± 7.9								21.6 ± 7.8
ARR13(AVG. ± SD)									14.0 ± 7.0								16.6 ± 6.6

Acknowledgements The authors would like to acknowledge the Australian Bureau of Meteorology for providing the pluviograph data used in this study. The authors would like to acknowledge the comments and suggestions by the reviewers, which have improved the quality of the manuscript.

References

Australia Bureau of Meteorology (BOM) (2016) How to use the AR and R87 IFD Tool. http://www.bom.gov.au/water/designRainfalls/ifd-arr87/howtoIFDTool.shtml. Accessed 10 Jan 2017
Australian Bureau of Statistics (BOM) (2013) Australia's climate. http://www.abs.gov.au. Accessed 10 Jan 2017
Ball J, Babister M, Nathan R, Weeks W, Weinmann E, Retallick M, Testoni I (2016) Australian rainfall and runoff: a guide to flood estimation. Commonwealth of Australia, Sydney
Bennett B, Lambert M, Asce AM, Thyer M, Bates BC, Leonard M (2016) Estimating extreme spatial rainfall intensities. J Hydrol Eng 21(3):04015074
Bernard MM (1932) Formulas for rainfall intensities of long duration. Trans ASCE 96(1801):592–624
Dourte D, Shukla S, Singh P, Haman D (2013) Rainfall intensity duration frequency relationships for Andhra Pradesh, India: changing rainfall patterns and implications for runoff and groundwater recharge. J Hydrol Eng 18(3):324–330
Du H, Xia J, Zeng S (2014) Regional frequency analysis of extreme precipitation and its spatio-temporal characteristics in the Huai River Basin, China. Nat Hazards 70:195–215
Elsebaie IH (2011) Developing rainfall intensity duration frequency relationship for two regions in Saudi Arabia. J King Saud Univ Eng Sci 24:131–140
Fréchet M (1927) Sur La Loi De Probabilité De L'écart Maximum. Journal of Annales De La Société Polonaise De Mathématique 6:93
Garcia-Urquia E (2016) Establishing rainfall frequency contour lines as thresholds for rainfall-induced landslides in tegucigalpa, honduras, 1980–2005. Nat Hazards 82:2107–2132
Green J, Xuereb K, Johnson F, Moore G, The C (2012) The revised intensity-frequency-duration (IFD) design rainfall estimates for Australia. In: An overview in proceedings of the 34th hydrology and water resources symposium, 19–22 November 2012, Sydney, Australia
Greenwood JA, Landwehr JM, Matalas NC, Wallis JR (1979) Probability weighted moments: definition and relation to parameters of several distributions expressible in inverse form. Water Resour Res 15:1049–1054
Greis NP, Wood EF (1983) Regional flood frequency estimation and network design. Water Resour 17(4):1167–1177
Gumbel EJ (1958) Statistics of extremes. Columbia University Press, New York
Haddad K, Rahman A (2014) Derivation of short-duration design rainfalls using daily rainfall statistics. Nat Hazards 74:1391–1401
Haddad K, Rahman A, Green J (2010) Design rainfall estimation in Australia: a case study using L-Moments and generalized least squares regression. Stoch Env Res Risk Assess 25(6):815–825
Haddad K, Rahman A, Green J, Kuczera G (2011) Design rainfall estimation for short storm durations using L-Moments and generalised least squares regression application to Australian Data. Int J Water Resour Arid Environ 1(3):210–218
Haddad K, Johnson F, Rahman A, Green J, Kuczera G (2015) Comparing three methods to form regions for design rainfall statistics: two case studies in Australia. J Hydrol 527:62–76
Hosking JR, Wallis J (1987) Parameter and quantile estimation for the generalized pareto distribution. Technometrics 29:339–349
Hosking JR, Wallis J (1997) Regional frequency analysis: an approach based on L-Moments. Cambridge University Press, New York, p 224
Hosking JR, Wallis J, Wood E (1985) Estimation of the generalized extreme value distribution by the method of probability weighted moments. Technometrics 27:251–261
Institution of Engineers Australia (I. E. Aust.) (1987) Australian rainfall and runoff: a guide to flood estimation. In: Pilgrim DH (ed) Engineers Australia, Canberra
Jakob D, Xuereb K, Taylor B (2007) Revision of design rainfalls over australia: a pilot study. Aust J Water Resour 11(2):153–159
Khan MZK, Sharma A, Mehrotra R, Schepen A, Wang QJ (2015) Does improved SSTA prediction ensure better seasonal rainfall forecasts? Water Resour Res 51(5):3370–3383
Kirkman TW (1996) Statistics to use: Kolmogorov–Smirnov test. College of Saint Benedict and Saint John's University. Accessed 10 Feb 2010

Landwehr J, Matalas N, Wallis J (1979) Probability weighted moments compared with some traditional techniques in estimating gumbel parameters and quantiles. Water Resour Res 15:1055–1064
Lee C, Kim T, Chung G, Choi M, Yoo C (2010) Application of bivariate frequency analysis to the derivation of rainfall frequency curves. Stoch Env Res Risk Assess 24:389–397
Liong S, Gautam T, Khu S, Babovic V, Keijzer M, Muttil N (2002) Genetic programming: a new paradigm in rainfall runoff modeling. J Am Water Resour As 38(3):705–718
Liu J, Doan C, Liong S, Sanders R, Dao A, Fewtrell T (2015) Regional frequency analysis of extreme rainfall events in Jakarta. Nat Hazards 75:1075–1104
Mamoon A, Joergensen NE, Rahman A, Qasem H (2014) Derivation of new design rainfall in qatar using L-moment based index frequency approach. Int J Sustain Built Environ 3:111–118
Millington N, Das S, Simonovic SP (2011) The comparison of GEV, Log-Pearson type 3 and Gumbel distributions in the Upper Thames River Watershed under Global Climate Models. Raziskovalno poročilo o vodnih sredstvih. London, Ontario, Canada, University of Western Ontario, Department of Civil and Environmental Engineering, p 52
Nhat LM, Tachikawa Y, Sayama T, Takara K (2006) Derivation of rainfall intensity duration frequency relationships for short duration rainfall from daily rainfall data. IHP Tech Doc Hydrol 6:89–96
Overeem A, Buishand A, Holleman I (2008) Rainfall depth duration frequency curves and their uncertainties. J Hydrol 348:124–134
Preacher KJ (2001) Calculation for the Chi square test: an interactive calculation tool for Chi Square tests of goodness-of-fit and independence [Computer Software]. http://quantpsy.org. Accessed 10 Jan 2017
Scholz FW, Stephens MA (1987) K sample Anderson darling tests. J Am Stat As 82:918–924
Verdon-Kidd DC, Kiem AS (2015) Regime shifts in annual maximum rainfall across Australia-implications for intensity-frequency-duration (IFD) relationships. Hydrol Earth Syst Sci 19:4735–4746
Wallis JR (1980) Risk and uncertainties in the evaluation of flood events for the design of hydraulic structures. In: Guggino E, Rossi G, Todini E (eds) Piene e Siccità. Fondazione Politecnica del Mediterraneo, Catania, pp 3–36
Weibull W (1951) A statistical distribution function of wide applicability. J Appl Mech Trans ASME 18(3):293–297
Xu Y, Tung Y (2009) Constrained scaling approach for design rainfall estimation. Stoch Env Res Risk Assess 23:697–705
Yilmaz AG, Hossain I, Perera BJC (2014) Effect of climate change and variability on extreme rainfall intensity–frequency–duration relationships: a case study of Melbourne. Hydrol Earth Syst Sci 18:4065–4076
Yu PS, Yang TC, Lin CS (2004) Regional rainfall intensity formulas based on scaling property of rainfall. J Hydrol 295:108–123